

## Water characteristics and transport of the Antarctic circumpolar current in the Indian Ocean

P M MURALEEDHARAN and BASIL MATHEW\*

National Institute of Oceanography, Dona Paula 403 004, India

\*Naval Physical and Oceanographic Laboratory, Cochin 682 004, India

MS received 14 April 1988; revised 22 August 1988

**Abstract.** Geostrophic velocities are computed across meridians 37°E and 105°E using hydrographic data. The estimated mass transport is represented on a temperature–salinity diagram. The characteristics of the water within the Antarctic circumpolar current at 37°E and 105°E are discussed. The computed transport agrees with the previous estimates. Transports due to the current between 45°S and the Antarctic continent at these two meridians are comparable. The westerly flow south of 42°S at 105°E is associated with a cyclonic eddy which appears to be a permanent feature, whereas the one at 50°S is related to the topography of the region.

**Keywords.** Antarctic circumpolar current; mass transport; bivariate distribution; Indian Ocean.

### 1. Introduction

The Antarctic circumpolar current (ACC) is the only ocean current circling the entire globe. Although the average speed of this eastward current is much lower (approximately 15 cm/s) than that of the equatorial currents, it transports a large amount of water because of its considerable horizontal and vertical extents. From geostrophic computations and direct current measurements it is well established that the ACC extends down to the bottom of the ocean (Callahan 1971). Attempts have been made in the past to estimate the net transport of the ACC by assuming geostrophic balance (Sverdrup *et al* 1942; Jacobs and Georgi 1977; Nowlin *et al* 1977) and by direct measurements. The direct measurements were mostly made in the Drake Passage (Reid and Nowlin 1971; Nowlin *et al* 1977; Whitworth *et al* 1982; Whitworth 1983) and along a section south of Australia (Callahan 1971). However, very little effort was made to study the modal properties of the waters carried by the ACC. In the present study, we have tried to find out the geostrophic transport across two sections in the Indian Ocean and represent it in bivariate classes of potential temperature and salinity.

### 2. Material and method

Two hydrographic sections consisting of 26 stations were used for the present study. The western section at 37°E was covered by the research vessel *Robert D Conrad* during its 17th cruise in March 1974, while the one at 105°E was covered in November 1971 by the US vessel *Eltanin*. The station locations are given in figure 1. The western section at

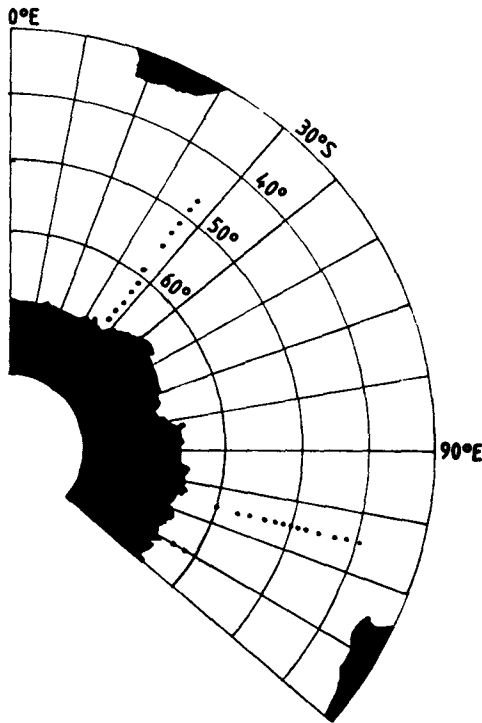


**Figure 1.** Track chart and station positions.

37°E represents only a part of the ACC. As the section at 105°E extends only up to 60°S, two additional stations to the south of 60°S were taken along 120°E. The latter were covered in the same cruise. It was assumed that this would not cause any appreciable error as the ACC is fairly steady south of the polar front (PF).

The geostrophic velocities were computed between station pairs relative to the deepest common observed depths following Callahan (1971) (figures 2 and 3). Vertical sections of potential temperature, salinity and geostrophic velocity were used for computing the transport and representing it in bivariate classes of potential temperature and salinity. In order to get the minute details, classes of potential temperature and salinity were chosen with smaller intervals, of 0.5°C and 0.1‰ respectively. The transports were computed through each solenoid formed by potential temperature and station pairs and integrated to get the total transport. This is achieved by superimposing potential temperature and salinity diagrams. The transport (flux) in each solenoid is differentiated again with respect to salinity in order to represent it on a temperature–salinity (T–S) diagram.

Figures 4 and 5 represent the net transport in bivariate classes of potential temperature (0.5°C intervals) and salinity (0.1‰ intervals). This method has the added advantage of giving the properties of the waters carried by the current and their contribution to the net flux.

To facilitate easy comparison, the geographical boundaries are chosen in such a way that the domains west of 50°E and east of 90°E represent, respectively, the western and eastern regions of the Indian Ocean sector of the Southern Ocean.

### 3. Results and discussion

#### 3.1 The current structure

Vertical sections of geostrophic currents across the two sections ( $37^{\circ}\text{E}$  and  $105^{\circ}\text{E}$ ) are shown in figures 2 and 3. The velocity structure across  $37^{\circ}\text{E}$  (figure 2) shows a weak zonal eastward component between  $55^{\circ}\text{S}$  and  $60^{\circ}\text{S}$  in the upper 1500 m. Beyond  $60^{\circ}\text{S}$  it goes on decreasing, and the flow becomes westward south of  $67^{\circ}\text{S}$ . The eastward flow is separated into two distinct zones: a narrow high-velocity core ( $> 15\text{ cm/s}$ ) just south of the India–Antarctica Ridge and the less intense belt further south (near  $57^{\circ}\text{S}$ ) already mentioned. At the surface, the polar front is located north of  $50^{\circ}\text{S}$ . Lutjeharms (1985) observed that the polar front was around  $50^{\circ}\text{S}$  in the western Indian Ocean. Here the maximum velocity exceeds  $15\text{ cm/s}$ . The westward flow is confined to the extreme southern boundary of the section. This suggests a narrow and weak contribution from

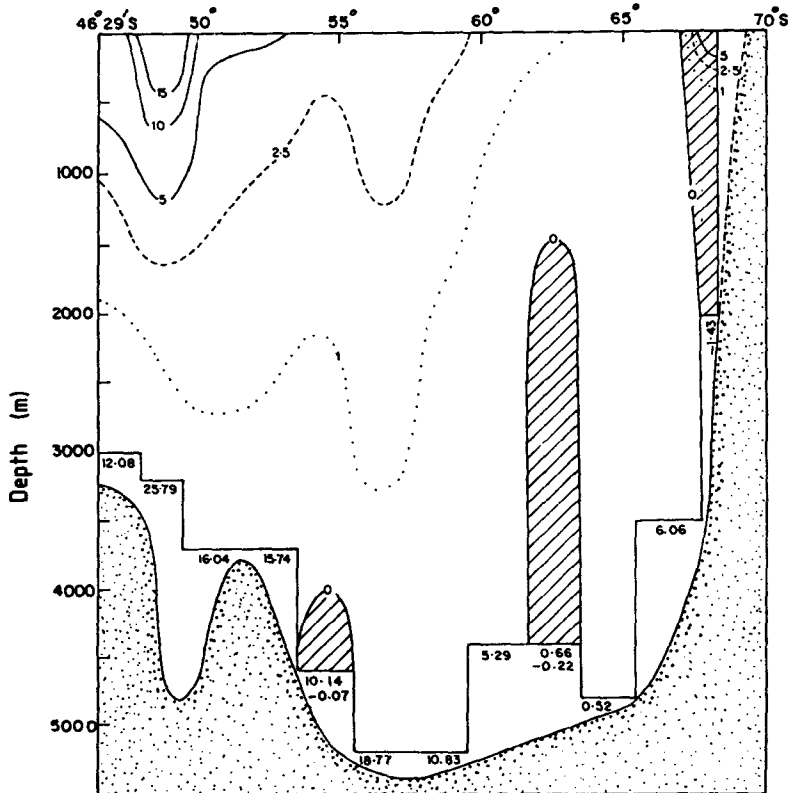


**Figure 2.** Geostrophic flow and transport across  $37^{\circ}\text{E}$  relative to the greatest common observed depths. Straight horizontal lines show the greatest common observed depth for station pairs. Westward flows are hatched and velocity contours are shown by solid lines for velocities at  $5\text{ cm/s}$  intervals and dashed/dotted lines for velocities with smaller intervals between them. Quantities of mass transport ( $10^6\text{ m}^3\text{ s}^{-1}$ ) between station pairs are shown below the horizontal lines. Positive and negative values indicate eastward and westward transports respectively. Negative transports, being insignificant, are not counted in the 50% and 75% boundaries.

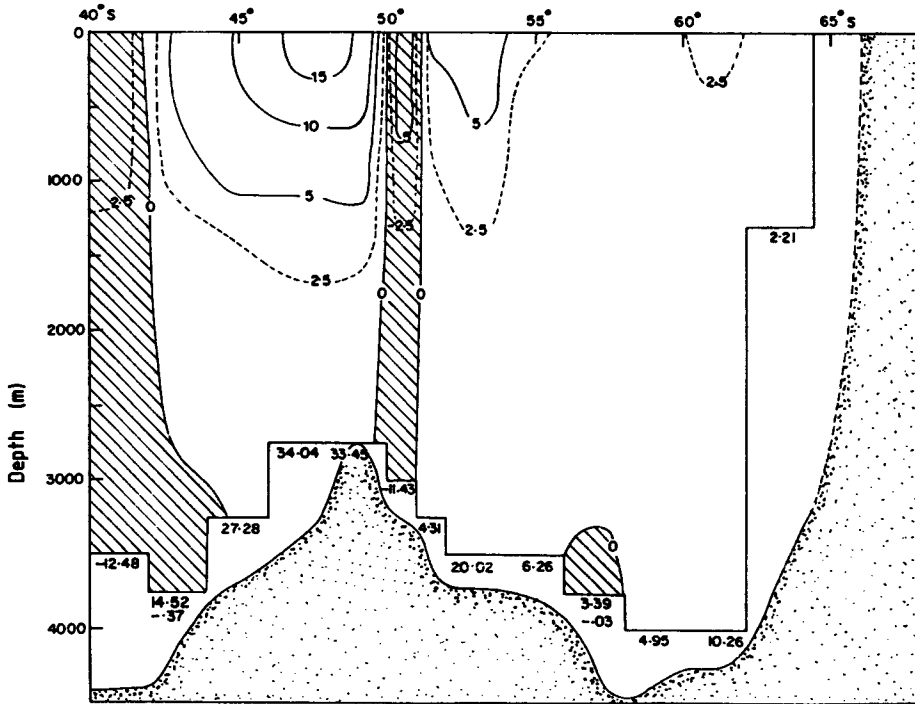


Figure 3. Geostrophic flow and transport across 105°E relative to the greatest common observed depths. See legend to figure 2 for details.

the east wind drift in this region. The zone of the Antarctic front is thus situated roughly around 67°S, slightly south of the position observed by Lutjeharms (1985).

A sub-Antarctic front (SAF) and a polar front are observed in the eastern section (figure 3). A westward flow, which separates these two fronts, extends down to the crest of the India–Antarctica Ridge. Callahan (1971) also found the same feature. He suggested that the zone over the ridge was characterized by extremely weak vertical shear throughout the water column. This could result in a westward flow or vanishing of the zonal component. The dynamics behind the westward countercurrent embedded in the ACC exactly over the India–Antarctica Ridge are still unknown. Callahan (1971) believed that the ACC was affected by major topographic features. According to him the position of the countercurrent is an indication of the influence of topography on the upper westward flow. He also felt, however, that the part played by the wind stress distribution could not be ignored. Interestingly, the zone of maximum westerly winds in the southern ocean (50°S) exactly coincides with the latitude of the countercurrent (Von Arx 1957). This strengthens the case for a topographic influence on the westward flow. Quoting Sverdrup *et al* (1942), Callahan (1971) pointed out that large-scale meanders in the ACC have been observed repeatedly over the meridional ridge system. This can be explained qualitatively by the conservation of potential vorticity (Pond and Pickard 1983), but a more complete dynamical model will help one to understand the real cause of this westward flow.

The westward flow at 40°S (figure 3) could be associated with a cyclonic eddy. Its

presence has been confirmed between Antarctica and the region south of Australia by Sarchenko *et al* (1978). A similar cyclonic circulation was noticed in the vicinity of the polar front at the Drake Passage by Joyce and Patterson (1977). Wyrтки (1962) observed a cyclonic circulation between 105°E and 110°E, centred at 35°S all along the depths that were investigated. This appears to be a permanent feature.

Thus, the net eastward flux of the ACC is mostly derived from the sub-Antarctic zone (SAZ) and the polar frontal zone (PFZ). The contribution of SAZ is the more dominant of the two. The core velocities of these two zones are 15 and 5 cm/s respectively. A less intense belt is also seen around 61°S, which could be either an extension of the PFZ or the Antarctic zone (AZ).

From the data collected during the *Melville*, *Yelcho* and *Atlantis II* cruises Whitworth *et al* (1982) calculated the maximum velocity of the ACC in both SAF and PF and the values exceed 40 cm/s. However, such high velocities could not be seen along 132°E, at 115°E (Callahan 1971), or along 145°E (Sverdrup 1940), where the velocities were less than half the values reported by Whitworth *et al* (1982). In the present study, the velocity of the ACC never exceeded 20 cm/s. The high velocity at the Drake Passage was mainly due to the narrowness of the path of the ACC.

### 3.2 Transport

The zonal transports computed within the ACC across 37°E and 105°E amount to  $122 \times 10^6 \text{ m}^3 \text{ s}^{-1}$  and  $160 \times 10^6 \text{ m}^3 \text{ s}^{-1}$  respectively. The excess transport at 105°E may be attributed to the greater meridional coverage of this section compared to that at 37°E; otherwise, both the values are comparable. The westward flux is more conspicuous in the eastern section, while it is almost absent to the west.

The previous measurements of transport within the ACC in all the three sectors of the southern ocean correlate well with the present estimates. Nowlin *et al* (1977) computed a transport of  $124 \times 10^6 \text{ m}^3 \text{ s}^{-1}$  across the Drake Passage and his estimate is comparable with that of Whitworth (1983), who estimated an average transport of  $121 \times 10^6 \text{ m}^3 \text{ s}^{-1}$  from a 370-day current record. Bryden and Pillsbury's (1977) estimate of  $262 \times 10^6 \text{ m}^3 \text{ s}^{-1}$  at the Drake Passage (based on one year's records from 6 m) deviates considerably from the normal value and the extremes, according to Nowlin *et al* (1977), might have been the result of a longer observation period.

The present estimates of  $122 \times 10^6 \text{ m}^3 \text{ s}^{-1}$  at 37°E and  $160 \times 10^6 \text{ m}^3 \text{ s}^{-1}$  at 105°E are supported by the values of Jacobs and Georgi (1977) and Callahan (1971). Jacobs and Georgi have calculated the transport between Cape Agulhas and Antarctica and these values slightly exceed the present ones, while Callahan's estimates at 115°E and 132°E are  $149 \times 10^6 \text{ m}^3 \text{ s}^{-1}$  and  $156 \times 10^6 \text{ m}^3 \text{ s}^{-1}$  respectively.

### 3.3 Bivariate distribution of the flux

The distribution of the total transport among classes of potential temperature (0.5°C intervals) and salinity (0.1‰ intervals) is shown in figures 4 and 5. The transport values enclosed by the solid lines are of those classes that together contribute 50% of the total transport and are said to be within the 50% boundary. Similarly the 75% boundary (dashed lines) is defined as that which encloses transport values of classes that contribute 75% of the total transport. The following are the numbers of classes enclosed by the 50% and 75% boundaries in the western and eastern regions.

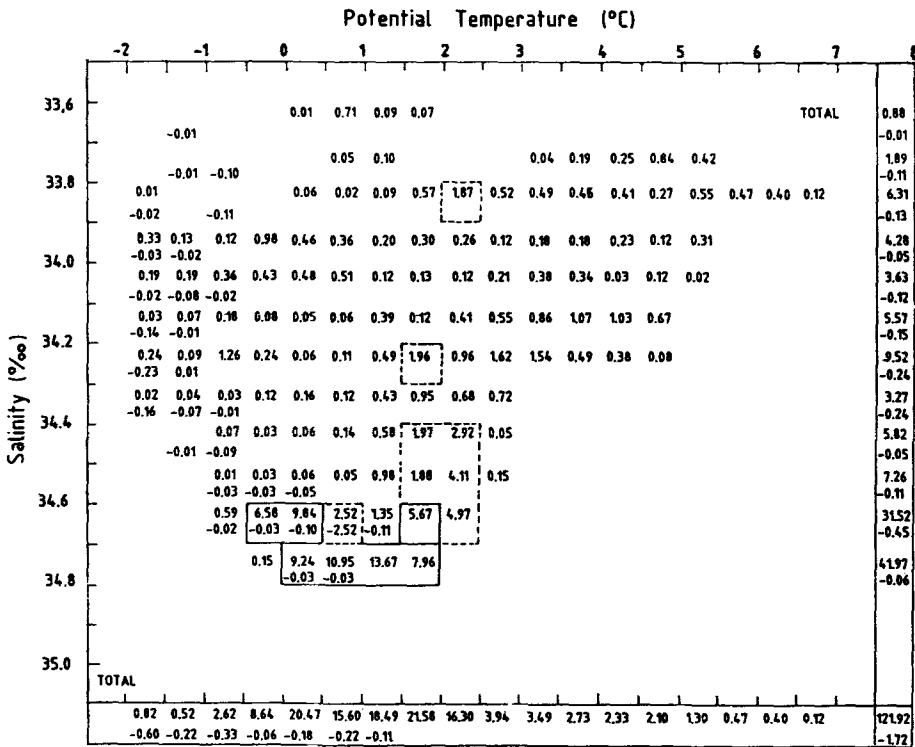


Figure 4. Distribution of the total transport across 37°E in bivariate classes of potential temperature and salinity. The solid-line boundary encloses classes that together contribute 50% of the total transport; the dashed-line boundary encloses classes that contribute 75%. The totals at bottom give distribution by potential temperature and those at right distributions by salinity. The total in the box in the bottom right-hand corner gives total transport ( $10^6 \text{ m}^3 \text{ s}^{-1}$ ) across 37°E. Negative values indicate westward transport.

Region	50%	75%
Western (figure 4)	7	15
Eastern (figure 5)	12	31

The two regions can be compared with regard to the number of classes enclosed by the 50% and 75% boundaries. Both 50% and 75% boundaries reveal that the eastern region of the southern Indian Ocean is more heterogeneous than the western region. Along 105°E the primary, secondary and tertiary modes are very prominent, both at the 50% and 75% levels, and are widely scattered throughout the water column (figure 5). At 37°E, 75% of the circumpolar current has a salinity  $> 34.2\text{‰}$  and a potential temperature ranging from  $-0.5^\circ\text{C}$  to  $2.5^\circ\text{C}$ . The highly saline primary mode within the 50% boundary has only 7 classes while the additional 25% includes 8 classes, probably because of the admixture of water mass from the north (figure 4). Similar mixing of water masses is also inferred at the eastern region from the additional 19 classes within the 75% boundary. It is also presumed that the water in this region is comparatively stratified.

The less saline ( $< 34.3\text{‰}$ ) warm water ( $3\text{--}7^\circ\text{C}$ ) noticed in the ACC at 37°E (figure 4) can be attributed to the southward advection of the Agulhas current. This accounts for

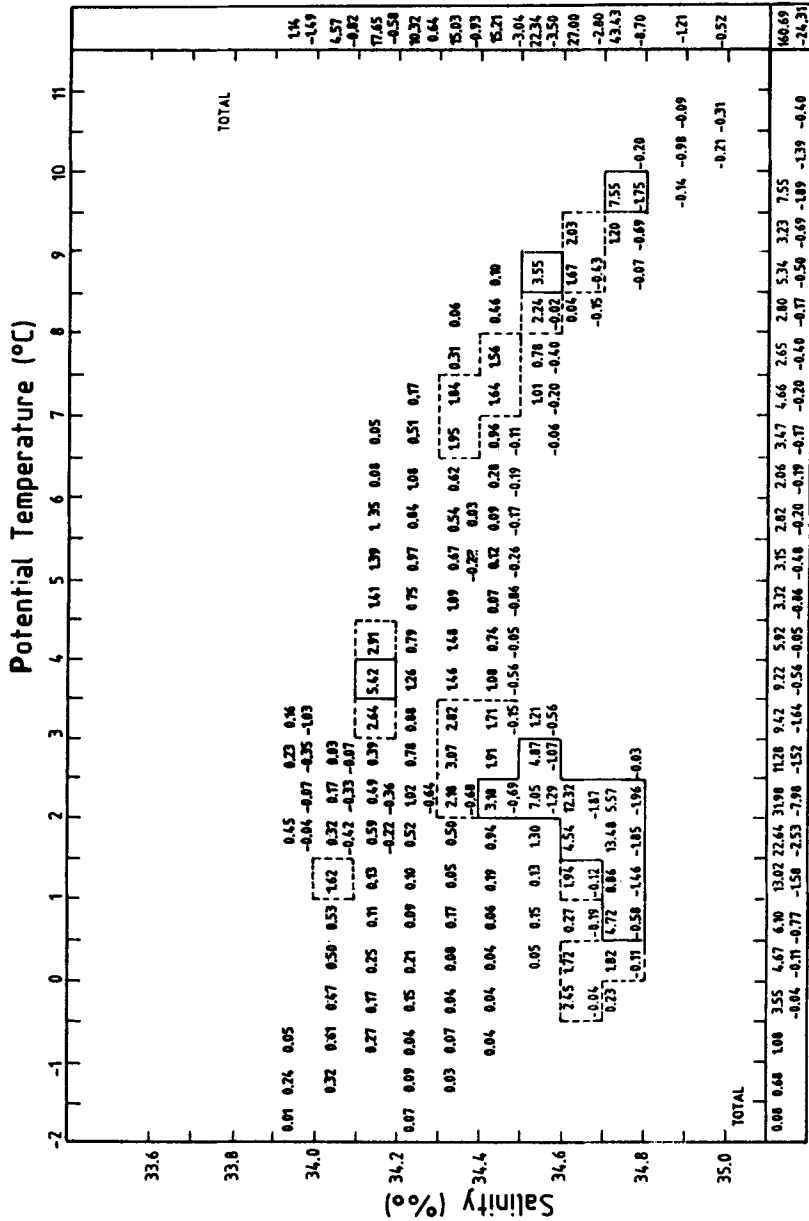


Figure 5. Distribution of the total transport across 105°E. See legend to figure 4 for details.

about 10% of the total volume transport in the ACC. Grundlingh (1978), using a satellite-tracking device, observed a southerly flow in the Agulhas current around 37°E and thought it to be the recycling of the Agulhas current. He could also locate the rapid eastward return of the Agulhas current west of 20°E and its path towards the east along 40°S. Therefore the warm, less saline water at 37°E and 45°S in the present section must be due to the influence of the Agulhas current. Similarly, the presence of saline water within the potential temperature range 7–11°C at 105°E (figure 5) is a clear evidence of the northward-flowing West Australian current. The secondary mode within the 50% level occupies this part of the current. There is an indication of this northward current in the figures of Hamon (1965) for the period October 16 to November 15 1960. An analogous current structure was observed by Wyrki (1957) and Rochford (1969) at the extreme west and east of the Indian Ocean sector of the Southern Ocean during the Austral summer.

#### 4. Conclusions

In the present study the velocity of the ACC never exceeded 20 cm/s. Two westward flows were noticed at 50°S and 40°S across the meridian 105°E. The westward flow at 40°S was found to be associated with a cyclonic eddy. The computed geostrophic transport across 37°E and 105°E amounts to  $122 \times 10^6 \text{ m}^3 \text{ s}^{-1}$  and  $160 \times 10^6 \text{ m}^3 \text{ s}^{-1}$  respectively. The distribution of the total transport in bivariate classes of potential temperature and salinity indicates that the eastern region of the Southern Ocean is more heterogeneous than the western region. The influence of a less saline Agulhas current and a saline West Australian current may be inferred from the frequency distribution.

#### References

- Bryden H L and Pillsbury R D 1977 Variability of deep flow in the Drake Passage from year-long current measurements; *J. Phys. Oceanogr.* **7** 803–810
- Callahan J E 1971 Velocity structure and flux of the Antarctic circumpolar current south of Australia; *J. Geophys. Res.* **76** 5859–5864
- Grundlingh M L 1978 Drift of a satellite-tracked buoy in the southern Agulhas current and Agulhas return current; *Deep Sea Res.* **25** 1209–1224
- Hamon B V 1965 Geostrophic current in the southeastern Indian Ocean; *Aust. J. Mar. Freshwater Res.* **16** 255–271
- Jacobs S S and Georgi D T 1977 Observations on the southwest Indian/Antarctic Ocean. In *A voyage of discovery* (ed.) M. Angel (Oxford: Pergamon Press) pp. 43–84
- Joyce T M and Patterson S L 1977 Cyclonic ring formation at the polar front in the Drake Passage; *Nature (London)* **265** 181–233
- Lutjeharms J R E 1985 Location of frontal systems between Africa and Antarctica: some preliminary results; *Deep Sea Res.* **32** 1499–1509
- Nowlin W D, Whitworth T III and Pillsbury R D 1977 Structure and transport of the Antarctic circumpolar current at Drake Passage from short-term measurements; *J. Phys. Oceanogr.* **7** 768–802
- Pond S and Pickard G 1983 *Introductory dynamical oceanography* (Oxford: Pergamon Press) p. 329
- Reid J L and Nowlin Jr W D 1971 Transport of water through the Drake Passage; *Deep Sea Res.* **18** 51–64
- Rochford D J 1969 Seasonal variations in the Indian Ocean along 110°E. 1. Hydrological structure of the upper 500 m; *Aust. J. Mar. Freshwater Res.* **13** 1–17
- Sarchenko V G, Emery W J and Vladimirov D A 1978 A cyclonic eddy in the Antarctic circumpolar



- current south of Australia. Results of Soviet–American observations aboard RV Professor Zubov; *J. Phys. Oceanogr.* **8** 825–837
- Sverdrup H O 1940 British, Australian, New Zealand Antarctic research expedition: Hydrology discussion; BANZARE Report Ser. A, Vol. 3, part 2, sect. 2
- Sverdrup H U, Johnson M W and Fleming R H 1942 *The oceans* (Englewood Cliffs NJ, USA: Prentice-Hall) pp. 1087
- Von Arx W 1957 An experimental approach to problems in physical oceanography. In *Physics and chemistry of the earth* (eds) L H Ahrens, F Press, K Rankama and S K Runcorn (New York: Pergamon Press) Vol. 2, p. 1
- Whitworth T III 1983 Monitoring the transport of the Antarctic circumpolar current at Drake passage; *J. Phys. Oceanogr.* **13** 2045–2057
- Whitworth T III, Nowlin Jr W D and Worly S J 1982 The net transport of the Antarctic circumpolar current through Drake Passage; *J. Phys. Oceanogr.* **12** 960–971
- Wyrтки K 1957 Die zirkulation an der oberfläche der südostasiatischen gewässer; *Dt. Hydrog. Z.* **10** 1–13
- Wyrтки K 1962 Geopotential topographies and associated circulation in the southeastern Indian Ocean; *Aust. J. Mar. Freshwater Res.* **13** 1–17